Advances in Physics Theories and Applications
ISSN 2224-719X (Paper) ISSN 2225-0638 (Online)
Vol.27, 2014


# Influence of Vortex-Antivortex Annihilation on the Potential Curve for Josephson Junction Based on The Modified Time Dependent Ginzburg-Landau Equations

Hari Wisodo[1, 2, *], Arif Hidayat[1], Pekik Nurwantoro[2], Agung Bambang Setio Utomo[2], Eny Latifah[1]

1. University of Gadjah Mada (UGM), Jl. Bulaksumur, Yogyakarta 55281, Indonesia
2. State University of Malang, Jl. Semarang 5, Malang 65145, Indonesia

* E-mail of the corresponding author: hari.wisodo.fmipa@um.ac.id

**Abstract**

The dynamics of annihilation a vortex-antivortex (VAV) pair in a Josephson junction has been investigated based on the modified Time Dependent Ginzburg Landau (TDGL) equations. The pair was generated only by the current-induced magnetic field. As the external current density is passed on the sample, a VAV enters the scene, moves toward the centre of the Josephson junction (JJ), and finally the pair is annihilated. The supercurrent density topology, order parameter topology, and voltage curve were also calculated. The influence of the dynamics of annihilation a VAV pair on the potensial curve is discussed.

**Keywords:** annihilation, anti vortex, Josephson junction, superconductor, vortex, voltage

## 1. Introduction

Applying type-II superconductors in a Josephson junction (JJ) can increase performance of the device because a type-II superconductors has higher critical magnetic field than a type-I superconductors. As a result, vortices can penetrate into the JJ when applied an external magnetic field **H** between the first critical magnetic field $H_{c1}$ and the second critical magnetic field $H_{c2}$. The vortex dynamics in the JJ when applied external current density produce an energy dissipation released in the form of a potential. Therefore, relation between the potential characteristics and the mechanisms of energy dissipation caused by vortex dynamics becomes very important for the application of JJ. Standard text books (Orlando and Delin, 1991; Tinkham, 1996) showed that the potential characteristics of the JJ has been well described by the model RCSJ (Resistively and Capacitively Shunted Junction). Because it is based on a simple circuit analysis, the RCSJ model can not be used to explain the mechanism of energy dissipation caused by vortex dynamics.

The modified Time Dependent Ginzburg-Landau (TDGL) equations has been successfully used by researchers to show the vortex dynamics in JJ-SNS (Superconductor-Normal-Superconductor). However, several fundamental questions, in particular, the influence of the annihilation dynamics of a vortex-antivortex (VAV) pair on the potential curve in the JJ-SNS remain open. The vortex or antivortex can be identified through a vector field of the supercurrent density $\mathbf{J}_s$ and the local magnetic induced $\mathbf{h} = \nabla\times\mathbf{A}$ where $\mathbf{A}$ is the magnetic vector potential (Wisodo et al., 2013). This study is based on the numerical solution of the modified TDGL equations.

## 2. Model

### *2.1 Modified TDGL Equations*

In the modified Ginzburg-Landau model, a dynamics state of a JJ-SNS is described by the order parameter $\Psi = (n_s)^{1/2}\exp(i\theta)$, where $i = \sqrt{-1}$, $\theta$ is the phase of the order parameter, $n_s$ is a Cooper pairs density, and the magnetic vector potential $\mathbf{A}$. Both $\Psi$ and $\mathbf{A}$ are a solution of the modified TDGL equations. The dimensionless forms of the equations are (Du and Remski, 2002; Du et al., 1995; Chapman et al., 1995)

$$\partial_t\Psi = (\nabla - i\mathbf{A})^2\Psi + (1-T)(1-|\Psi|^2)\Psi \text{ and } \sigma\partial_t\mathbf{A} = \mathbf{J}_s - \kappa^2\nabla\times\nabla\times\mathbf{A} \text{ for } \Omega_s \quad (1)$$

$$\partial_t\Psi = m(\nabla - i\mathbf{A})^2\Psi + \alpha\Psi \text{ and } \sigma\partial_t\mathbf{A} = m\mathbf{J}_s - \kappa^2\nabla\times\nabla\times\mathbf{A} \text{ for } \Omega_n \quad (2)$$

 

where the potential gauge is chosen equal to zero, $\Omega_s$ is superconductive region, $\Omega_n$ is normal region (Fig. 1.a). The expression of the supercurrent density is given by $\mathbf{J}_s = (1-T)(\nabla\theta - \mathbf{A})|\Psi|^2$ where $T$ is the temperature. The normal current density is given by Ohm's law $\mathbf{J}_n = \sigma\partial_t\mathbf{A} = \sigma\mathbf{E}$ where $\mathbf{E}$ is the electric field and $\sigma$ is the electric conductivity. In Eq. (1) and (2), lengths have been scaled in units of the coherent length at zero temperature $\xi_{GL}(0)$, time in unit of $\tau = \xi_{GL}^2(0)/D$ where $D$ is a phenomenological diffusion constant, $\Psi$ in unit of $\Psi_{0,GL}(0)(1-T)^{1/2}$, $\mathbf{A}$ in unit of $A_0 = \Phi_0/2\pi\xi_{GL}(0)$ where $\Phi_0 = 2\pi\hbar/e_s$ is the flux quantum, $\mathbf{B}$ in unit of $A_0/\xi_{GL}(0)$, $\Phi$ in unit of $D\Phi_0/2\pi\xi_{GL}^2(0)$, $\mathbf{H}$ in unit of $H_{c2}(0)$, $\mathbf{E}$ in unit of $E_0 = D\Phi_0/2\pi\xi_{GL}^3(0)$, $\sigma$ in unit of $\sigma_0 = 1/\mu_0 D\kappa^2$ where $\kappa = \lambda/\xi$ is the Ginzburg-Landau parameter. $T$ in unit of $T_c$, $\mathbf{J}$ in unit of $J_0 = H_{c2}(0)/\xi_{GL}(0)$, $m$ is related to the mass ratio of a superconducting electron and a normal electron.

*2.2 Model System*

A JJ-SNS sized $21\xi_{GL}(0)\times 10\xi_{GL}(0)$ with $\kappa = 1.3$ (niobium), $\sigma = 1$, $m = 1$, $\alpha = 1$ and $T = 0$ is placed in a vacuum without external magnetic field, Fig. 1.a. A normal sample width $1\xi_{GL}(0)$ as a junction is placed in the midle. This situation gives boundary condition for $\Psi$ in the form $(\nabla - i\mathbf{A})|_n = 0$. The external current density $\mathbf{J}_e = J_e\hat{\mathbf{i}}$ is passed on the superconductor by imposing an external magnetic field difference between the upper and lower boundaries (Machida and Kaburaki, 1993; Vodolazov and Peeters, 2007). The current-induced magnetic field at the upper and lower boundaries is given by $\mathbf{H}_t = H_z\hat{\mathbf{k}} = J_{e;x}L_y/(2\kappa^2)\hat{\mathbf{k}}$ and $\mathbf{H}_b = -\mathbf{H}_t$. This condition gives boundary conditions for $\mathbf{A}$, namely $\nabla\times\mathbf{A} = \mathbf{H}$ with $\mathbf{H} = 0$ at $x = 0$ and $x = L_x$, $\mathbf{H} = \mathbf{H}_t$ at $y = 0$, and $\mathbf{H} = \mathbf{H}_b$ at $y = L_y$. The boundary conditions on the superconductor-normal interface are $[\Psi] = 0$, $[\mathbf{A}] = 0$, $(\nabla\times\mathbf{A})\times\hat{\mathbf{n}} = 0$, $(\nabla - i\mathbf{A})\Psi\bullet\hat{\mathbf{n}}\big|_{\Gamma s} = m(\nabla - i\mathbf{A})\Psi\bullet\hat{\mathbf{n}}\big|_{\Gamma n}$ where $\Gamma_s$ is superconductor boundary and $\Gamma_n$ is normal material boundary. The voltage difference between $x = 0$ and $x = L_x$ caused by the VAV dynamics is calculated using $V(t) = \int_0^{L_x}\left[(1/L_y)\int_0^{L_y}(-d\mathbf{A}/dt)dy\right]dx$ (Machida and Kaburaki, 1994).

## 3. Method

The modified TDGL equations are discretized using the finite difference method where the Euler method is used to discretize time variable. *U*-Ψ method (Gropp et al., 1996) is used to preserve gauge invariance under discretization with the link variables $U_{\mu;i,j} = \exp(-iA_{\mu;i,j}h_\mu)$ for $\mu = x, y$ (Barba-Ortega et al., 2010; Bolech et al., 1995; Kaper and Kwong, 1995; Sardella et al., 2006; Vodolazov et al., 2003). The size of computational grid is chosen $N_x \times N_y = 210 \times 100$ where the size of the typical grid cell is $h_x \times h_y = 0.1\xi_{GL}(0) \times 0.1\xi_{GL}(0)$, see Fig. 1.b, and time step $\Delta t = 0.001\tau$ is chosen to fill a stability criterion, $\Delta t < (h_x)^2/2\kappa^2$ where $h_x = h_y$ (Winiecki and Adam, 2002). The evaluation points for $\Psi$, $A_x$, $A_y$ , $B_z$ at a typical grid cell $(x_i, y_j)$ are shown in Fig. 1.b.

## 4. Results and Discussion

*4.1. E-J Curve*

The result of the *E-J* characteristic curve for JJ-SNS is shown in Fig. 2. Based on the number of vortices that can penetrate into the JJ-SNS, in general, the curve can be divided into four regions, namely regions A, B, C and D. Vortices can not penetrate into the JJ-SNS in region A. In region B, a pair of VAV entered into JJ-SNS through the normal material. The vortex enter through the upper side and the anti-vortex enter through the bottom side. In region C, the three pairs of VAV entered into JJ-SNS, the two pairs in superconductive sampel and a pair in normal sample. In region D, the number of VAV pairs in JJ-SNS is larger than in region C. The $\mathbf{J}_e$ variations can cause the changes of number of VAV pairs that can penetrate into the JJ-SNS.

*4.2. VAV Dynamics in the JJ-SNS*

The density of external current $J_e = 0.20J_0$ cause a VAV pair entered into JJ-SNS through the normal sample. Fig. 3 show the VAV dynamics during in the JJ-SNS. The vortex entered from upper side and anti vortex entered from bottom side at $t = 12.2\tau$ (Fig. 3.a1). Both move closer to each other towards the centre of the sample (Fig. 3.b1, 3.c1). Finally, the vortex and antivortex annihilate each other at $t = 18.6\tau$ (Fig. 3.d1). The annihilation occurs periodically.

The increasing of the density of external current to be $J_e = 0.25J_0$ cause many more a VAV pair entered into JJ-SNS. Fig. 4 show a VAV dynamics during in the JJ-SNS. In normal sample, vortex penetrate from upper side and anti

 

vortex penetrate from bottom side at $t = 8.0\,\tau$ (Fig. 4.a). Both annihilate each other at $t = 11.4\,\tau$ (Fig. 4.b). After that, three vortex entered from upper side and three anti vortex entered from bottom side (Fig. 4.c). Because of the VAV pair in the normal sample moving faster than in the superconductor sample, these pair annihilate each other at $t = 21.8\,\tau$ (Fig. 4.d) and then two pairs of VAV in the superconductor sample annihilate each other at $t = 23.1\,\tau$ (Fig. 4.e). The annihilation occurs periodically.

So, the decreasing or increasing of the external current density can generate different numbers of VAV that can be entered into the JJ-SNS. The difference of this amount will make a difference of the VAV pair annihilation dynamics. The dynamics is associated with the dissipation of the energy released in the form of potential.

*4.3. Potential Curve*

Periodicity of the VAV annihilation in the JJ-SNS applied $J_e$=0.20$J_0$ and $J_e$=0.25$J_0$ is shown on the $V(t)$ curve in Fig. 5. It seem that the periodicity of the VAV annihilation in the JJ-SNS applied $J_e$=0.25$J_0$ is greater than the periodicity of the VAV annihilation in the JJ-SNS applied $J_e$=0.20$J_0$. The potential values for the VAV dynamics shown in Fig. 3 and 4 also can be seen in the Fig. 5. The sharp pulses (peak b, d, e, c1) appears during the vortex and antivortex annihilate each other. The same thing also happened to the VAV annihilation in the clean superconductors (Wisodo et al., 2013).

The external current density $J_e$ applied on the JJ-SNS will generate supercurrent density $J_s$ and normal current density $J_n$. Fig. 6 show the linkage between the VAV dynamics, the currents and the potential $V$ for $J_e = 0.25J_0$. There are the periodical small pulses (pulse b and d) and the periodical sharp pulses (pulse e). The small pulses arise because of the vortex and antivortex annihilate each other in the normal material, (Fig. 4.b and 4.d) and the sharp pulses arise because of the vortex and antivortex annihilate each other in the superconductor material (Fig. 4.e). The small pulses period is smaller than the sharp pulses period.

An average of the super current density $\langle J_s \rangle$, normal current density $\langle J_n \rangle$ and total current density $\langle J \rangle$ fluctuate as shown in Fig. 7 (bottom). The value of $\langle J_s \rangle$ and $\langle J_n \rangle$ is always less than $J_e$ and the $\langle J \rangle$ value is always greater than $J_e$. When there is annihilation VAV (pulse b, d, e), the sharp pulses only appear on the $\langle J_n \rangle$ curve. Vector field of the super current $\mathbf{J}_s$, normal current $\mathbf{J}_n$ and total current density $\mathbf{J}$ at $t = 17.8\,\tau$, pulse c in Fig. 6 (above), is shown in Fig. 7. The super current density circulate around vortex and antivortex in normal and superconductive material. The normal current density only circulate around vortex and antivortex in the normal material. Sum of vector field $\mathbf{J}_s$ and $\mathbf{J}_n$ produce a vector field $\mathbf{J}$ circulating around the vortex and anti-vortex in the superconductive materials.

## 5. Conclusion

Influence of the dynamics of annihilation VAV in the JJ-SNS has been successfully studied using modified TDGL equation. Variations of the external current density value can cause variations in the number of VAV pair penetrating into the JJ-SNS. As a result, the dynamics of vortex and anti-vortex also varies that give the effect on the characteristic curves $VI$ and $V(t)$. The sharp pulses on the $V(t)$ curve appears during the vortex and antivortex annihilate each other. Periodicity of the sharp pulse decreases with increasing of the external current density. Periodicity of the VAV annihilation in the normal material is smaller than in the superconductive material.

## Acknowledgements

We thank DP2M DIRJEN DIKTI KEMDIKBUD under contract No. 1196/UN32.14/LT/2013 for financial support of this project and DIKTI KEMDIKBUD that has provided assistance in the form of scholarships BPPS during the study.

## References

Orlando, T.P. dan Delin, K.A., 1991, *Foundation of Superconductivity*, Masachusetts: Addison-Wesley Publishing Company, Inc., p. 292, 233

Tinkham, M., 1996, *Introduction to Superconductivity*, New York: McGraw-Hill, Inc., hlm. 13, 202-205

 

Du, Q. dan Remski, J., 2002, Limiting Models for Josephson Junctions and Superconducting Weak Link, *Journal of Mathematical Analysis and Applications*, **266**, 357-382

Du, Q., Gunzburger, M.D., Peterson, J.S., 1995, Computational Simulation of Type II Superconductivity Including Pinning Phenomena, *Physical Review B*, **51**, 16194-16203

Chapman, S.J., Du, Q., Gunzburger, M.D., 1995, A Ginzburg-Landau Type Model of Superconducting/ Normal Junctions Including Josephson Junctions, *Europ. J. Appl.*, **6**, 97-114

Machida, M. dan Kaburaki, H., 1993, Direct simulation of the Time Dependent Ginzburg-Landau Equation for Type II Superconducting Thin Film: Vortex Dynamics and *V-I* Characteristics, *Physical Review Letter*, **71**, 3206-3209

Vodolazov, D.Y. dan Peeters, F.M., 2007, Rearrangement of the vortex lattice due to instabilities of vortex flow, *Physical Review B*, **76**, 014521

Machida, M. dan Kaburaki, H., 1994, Numerical simulation of flux-pinning dynamics for a defect in a type-II superconductor, *Physical Review B*, **50**, 2, 1286-1289.

Gropp, W.D., Kaper, H.G., Leaf, G.K., Levine, D.M., Palumbo, M., Vinokur, V.M., 1996, Numerical Simulation of Vorteks Dynamics in Type-II Superconductors, *Journal of Computational Physics*, **123**, 254-266.

Barba-Ortega, J., Becerra, A., Aguiar, J.A., 2010, Two Dimensional Vorteks Structures in a Superconductor Slab at Low Temperatures, *Physica C*, **470**, 225-230.

Bolech, C., Buscaglia, G.C., Lopez, A., 1995, Numerical Simulation of Vorteks Arrays in Thin Superconducting Films, *Physical Review B*, **52**, R15719-R15722.

Wisodo, H., Nurwantoro, P., Utomo, A.B.S., 2013, Voltage Curve for Annihilation Dynamics of A Vortex-Antivortex Pair in Mesoscopic Superconductor, *Journal of Natural Sciences Research*, **3**, 9, 140-146

 

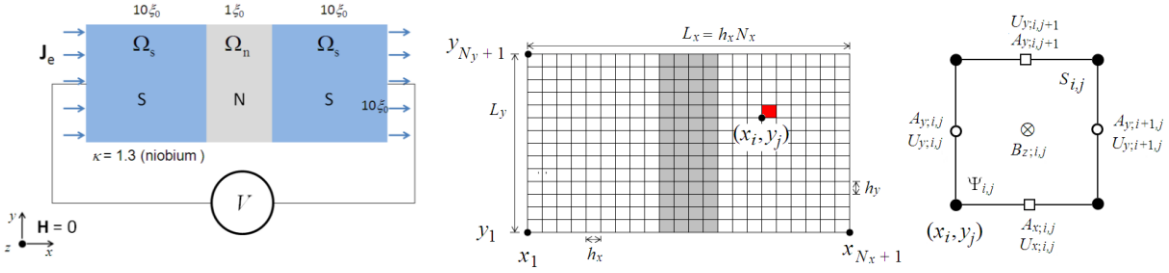


(a) (b)

Figure 1. Model system of the JJ-SNS (a) and the computational grid (b).

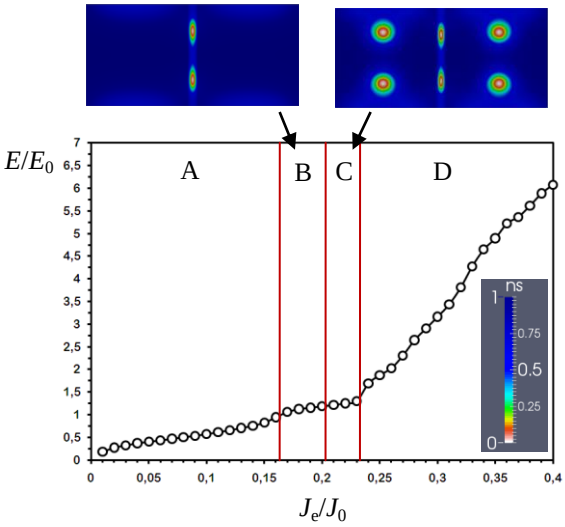


Figure 2. Characteristic curve *E-J* for JJ-SNS

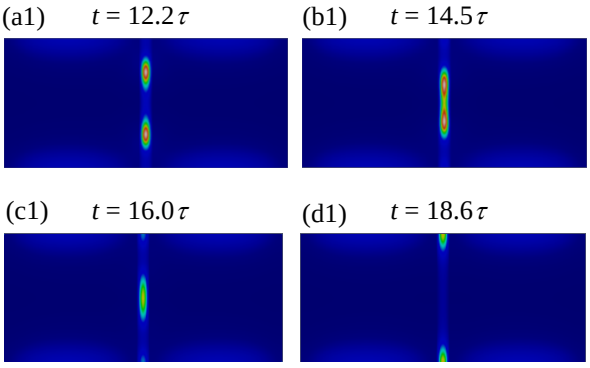


Figure 3. Countur of the super electron density $n_s$ of the JJ-SNS for $J_e = 0.20J_0$

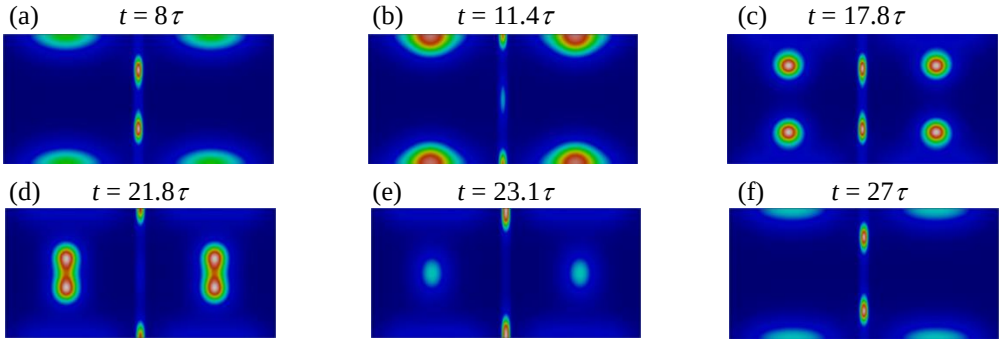


Figure 4. Countur of the super electron density $n_s$ of the JJ-SNS for $J_e = 0.25J_0$

 

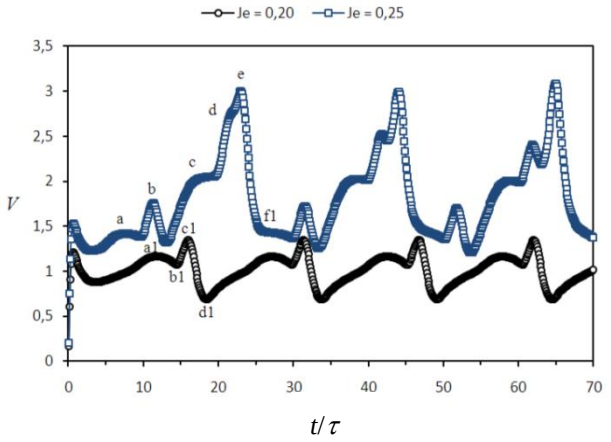


Figure 5. Potential $V$ as a function of time as the external current density $J_e = 0.20J_0$ and $J_e=0.25J_0$ passed into the JJ-SNS.

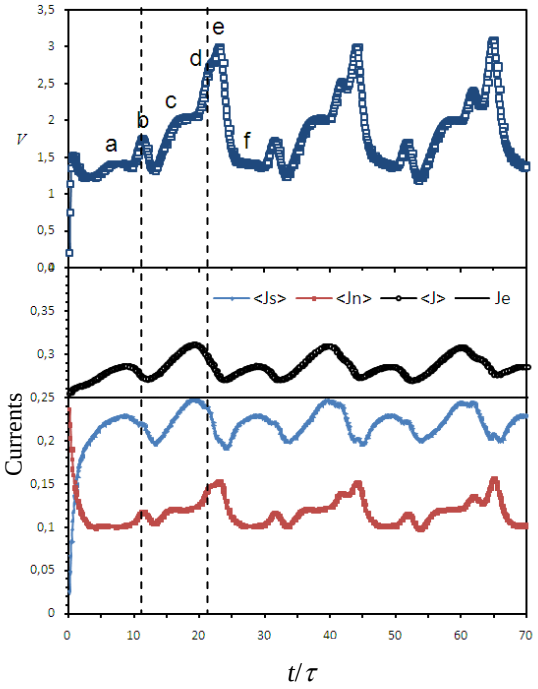


Figure 6. $V(t)$ curve (top), average of the $<J_s>$, $<J_n>$ and $<J>$ as a function of time (bottom) as the external current density $J_e=0.25J_0$ passed into the JJ-SNS.

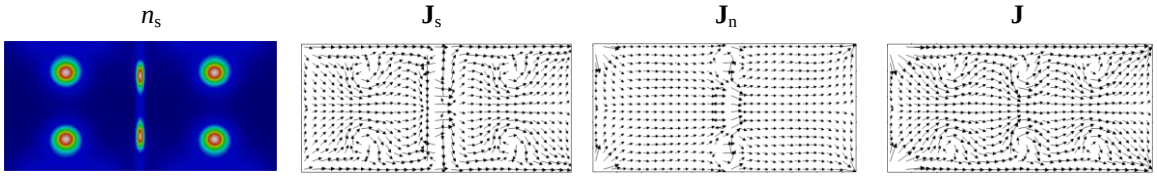


Figure 7. The super electron density $n_s$, vector field of the $\mathbf{J}_s$, $\mathbf{J}_n$ and $\mathbf{J}$ at $t = 17.8\tau$ as the external current density $J_e = 0.25J_0$ passed into the JJ-SNS.